

# Visual Servoing For Automatic and Uncalibrated Needle Placement For Percutaneous Procedures

Nassir Navab\*, Benedicte Bascle\*, Michael Loser\*, Bernhard Geiger\* and Russel Taylor\*

\*Siemens Corporate Research, Imaging & Visualization Department, Princeton, NJ, USA

♦ Siemens AG, Medical Engineering Group, Erlangen, Germany

♣NSF ERC, CIS-Lab, Johns Hopkins University, Baltimore, MD, USA

## Abstract

*This paper presents a new approach to image-based guidance of a needle or surgical tool during percutaneous procedures. The method is based on visual servoing. It requires no prior calibration or registration. The technique provides highly precise 3D-alignment of the tool with respect to an anatomic target. By taking advantage of projective geometry and projective invariants, this can be achieved in a fixed number (12) of iterations. In addition the approach estimates the required insertion depth. Experiments include automatic 3D alignment and insertion of a needle held by a medical robot into a pig kidney under X-ray fluoroscopy.*

---

**Keywords:** visual servoing, projective geometry, perspective invariant, cross-ratios, percutaneous procedures, needle placement

## 1. Introduction

Percutaneous surgical procedures are rapidly growing in popularity. Since they are less invasive than traditional open techniques, they significantly reduce patient recovery time and discomfort. However, during percutaneous procedures, the surgeon does not have a direct view of anatomic structures. Instead he/she must rely on indirect views provided by imaging modalities such as X-ray fluoroscopes. This is more challenging and requires the physician to be highly experienced. Successful targeting of an anatomic structure is dependent on the surgeon's skill, especially if the target is small.

To overcome this problem, several researchers proposed the use of robotic systems to assist in percutaneous procedures. The methods they propose all require time consuming pre-operative registration procedures between

robot, imaging system and the patient's anatomy [7] [8] [9].

In this paper we present a new method to image-based guidance of a needle or surgical tool in percutaneous procedures that requires no prior calibration or registration. The approach is based on visual servoing [4]. As far as the authors know, this is the first medical use of visual servoing [12]. We show that precise 3D-alignment of the tool to a target can be achieved by performing visual servoing of the tool in 3 successive planes using two different views. Visual servoing of the needle or tool in each plane is achieved using a new technique based on projective invariants. This technique converges in exactly three iterations, whereas "traditional" visual servoing techniques converge in an a-priori unknown number of iterations. The insertion depth required to reach the target is estimated using cross-ratios.

## 2. Needle Placement by Visual Servoing in 3 Successive Planes using 2 views

Our approach for 3D alignment of a needle or tool to a target is the following:

We assume imaging is provided by a simple uniplanar X-ray fluoroscope (C-arm). This is the imaging modality most commonly available in the operating room. Its imaging process is approximated by a pinhole camera model. The needle itself is manipulated by a mechanical device such as a passive or active robotic arm that allows arbitrary pivoting of the needle around its tip (see fig. 1 and 2). The surgeon chooses a fixed needle entry point  $F$  on the patient, and places the needle device in a way that its needle tip is located at that entry point. No calibration of the set-up or registration of the patient to the set-up is required.

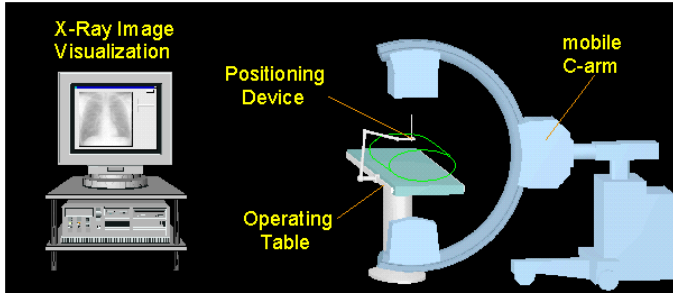


Figure 1 – Set-up: imaging is provided by a uniplanar X-ray fluoroscope (C-arm)

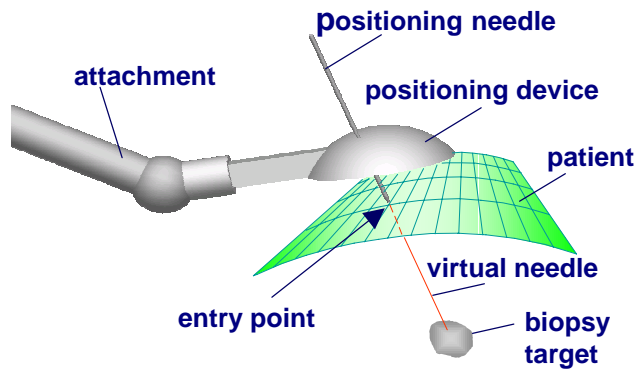


Figure 2 – Set-up: a mechanical device (passive or active robotic arm) holds the needle and allows arbitrary pivoting of the needle around its tip. The tip of the needle is placed at a fixed entry point by the surgeon.

The C-arm is then positioned, so that the target area and a part of the needle are both visible on the X-ray image. The surgeon defines the projection  $t$  of the 3D anatomical target  $T$  in the image. At the moment, we assume  $T$  remains static during the procedure.

First the mechanical device moves the needle in an arbitrary plane  $P_1$  containing  $F$  until the projection of the needle is aligned with the target  $t$  in the image (see fig. 3a). This can be performed in 3 iterations using a new visual servoing technique presented in the next section. The final position of the needle in plane  $P_1$  is called  $L_1$ .

The system repeats this process by choosing a second plane  $P_2$  containing  $F$ . The choice of  $P_2$  is arbitrary. In practice, the system takes  $P_2$  perpendicular to  $P_1$  for precision purposes. The needle is rotated in plane  $P_2$  until it is visually aligned to the target  $t$  in the image (see fig. 3b). This is done as previously by using

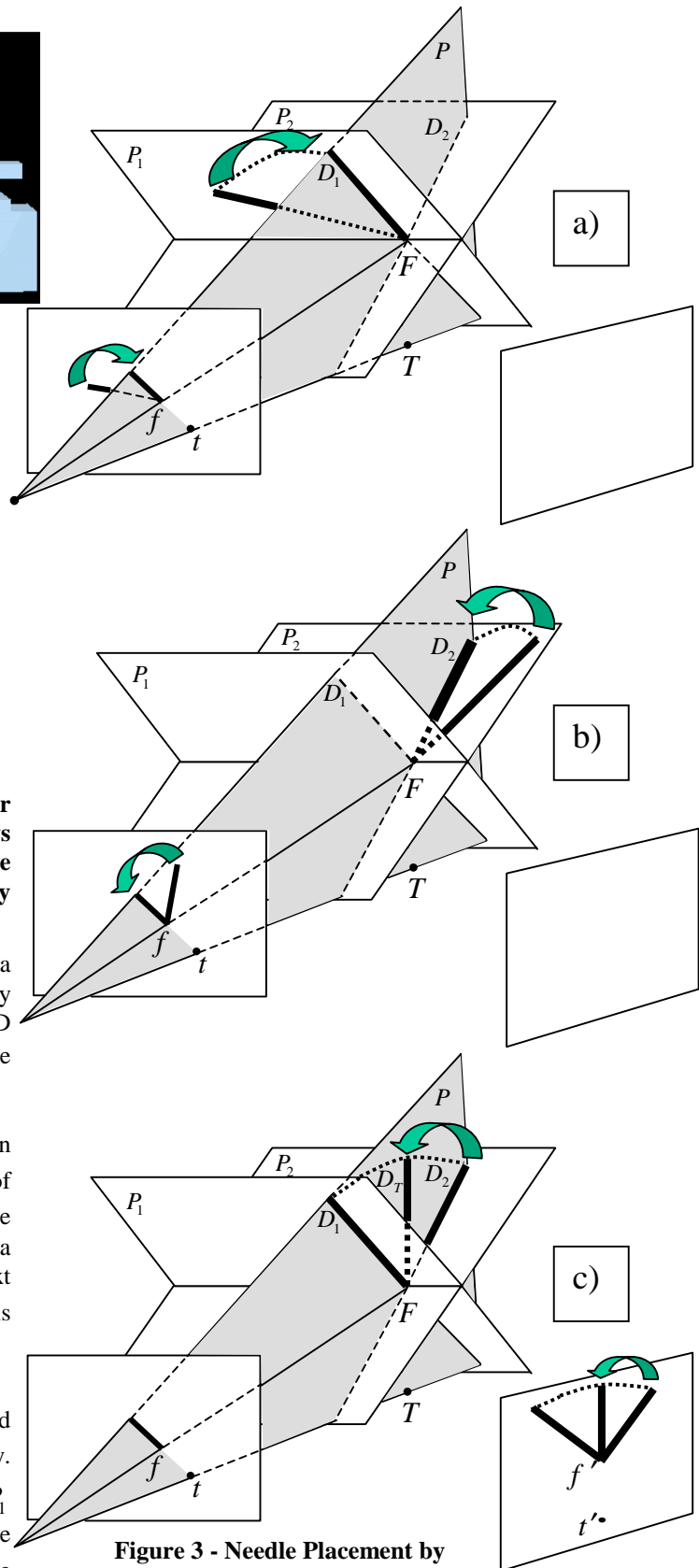


Figure 3 - Needle Placement by

Visual Servoing in 3 Successive Planes using 2 views

the visual servoing technique presented in section 3. The position of the needle that gives visual alignment is called  $L_2$ .

The positions of the needle  $L_1 \subset P_1$  and  $L_2 \subset P_2$  define a unique plane  $P$ , which contains the X-ray source, the target point  $T$  and the fixed entry point  $F$ . This is the maximum information we can get from a single viewpoint.

The physician needs to move the C-arm to a second viewing direction. The surgeon defines the projection  $t'$  of the 3D target point  $T$  in the new image. Now we move the needle only in the plane  $P$  until the needle is once again visually aligned to the target in the image (see fig. 3c). This is done using the visual servoing approach of section 3. This results in the final 3D alignment of the needle, the entry point and the anatomic target point. The needle is then ready to insert. The correctness of the alignment can also be checked by moving the C-arm to a third viewing direction.

### 3. Visual Servoing of a Needle in a plane using cross-ratios

In section 2 we showed how 3D alignment of a needle to a target can be achieved by performing visual servoing of the needle in three successive planes. Here we explain how the visual servoing of the needle in a plane is performed. This is a new technique based on projective invariants. It can be described as follows:

Let  $\Pi$  be the plane in which the needle is rotated, and  $F$  the fixed point around which the rotation is done. The initial orientation  $L_1$  of the needle in plane  $\Pi$  is arbitrary.  $T$  is the 3D target point.

An image  $I$  is taken of the scene. The 3D position  $L_1$  of the needle projects onto line  $l_1$  in the image. The position of  $l_1$  is detected and stored in memory.

The needle is rotated in plane  $\Pi$  around fixed point  $F$  by an arbitrary amount  $\theta_1$ . This brings it to position  $L_2$ . Another image is taken. The 3D line  $L_2$  projects onto 2D line  $l_2$  in the image. The position of  $l_2$  is detected and stored in memory.

The needle is rotated again by an angle  $\theta_2$ . This puts it into position  $L_3$ . Another image is obtained.  $L_3$  projects

onto  $l_3$  in the image.  $l_3$  is detected and its position stored in memory.

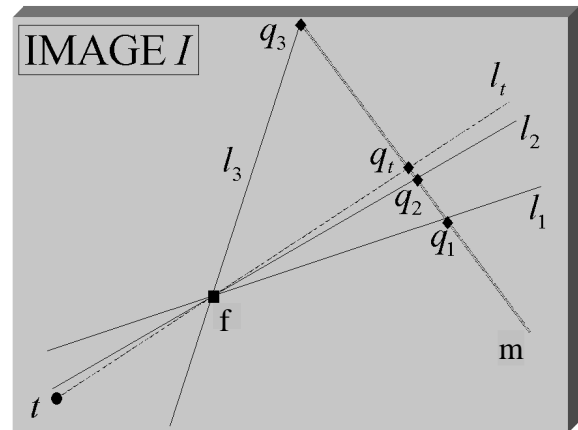
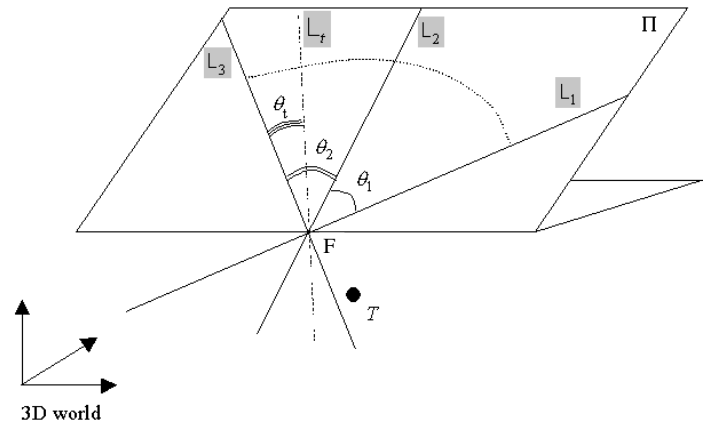


Figure 4 - Visual Servoing of a Needle in a plane using cross-ratios

The intersection point of  $l_1, l_2$  and  $l_3$ , denoted  $f$ , is determined by least squares. Note that  $f$  is the projection of the fixed point  $F$  around which the needle is rotated.

Let  $t$  be the projection of the 3D target  $T$  in the image. We assume  $t$  remains static during the procedure. The position of  $t$  is given interactively by the surgeon.

The line  $l_t = (ft)$  is constructed. Note that  $l_t$  is the 2D projection of the 3D position  $L_t$  of the needle that achieves visual servoing (e.g. the visual alignment of the needle and the target) and that we wish to estimate.

$l_1, l_2, l_3$  and  $l_t$  form a pencil of 2D lines. The cross-ratio  $c = (l_1, l_2, l_3, l_t)$  of these lines is calculated. This is done using an arbitrary line  $m$  that intersects all four lines. If  $q_1 = l_1 \cap m$ ,  $q_2 = l_2 \cap m$ ,  $q_3 = l_3 \cap m$  and  $q_t = l_t \cap m$  are the intersections of  $l_1, l_2, l_3, l_t$  with  $m$ , then

$$c = (l_1, l_2, l_3, l_t) = (q_1, q_2, q_3, q_t) \\ = (q_1 q_3 * q_2 q_t) \div (q_1 q_t * q_2 q_3)$$

Note that the value of  $c$  is invariant to the choice of the line  $m$ .

Cross-ratios are one of the invariants of projective geometry. Therefore the cross-ratio of a pencil of 3D lines is equal to the cross-ratio of the pencil of 2D lines formed by its perspective projections in an image. Therefore the cross-ratio  $(L_1, L_2, L_3, L_t)$  of the four 3D lines

$L_1, L_2, L_3$  and  $L_t$  is equal to  $c$ , e.g.

$$(L_1, L_2, L_3, L_t) = (l_1, l_2, l_3, l_t) = c.$$

From  $(L_1, L_2, L_3, L_t)$ , we estimate the angle

$\theta_t$  necessary to rotate the needle from position  $L_3$  to  $L_t$ .

The formula for  $\theta_t$  comes from the relationship between the cross-ratio of four lines and the angle between these lines. This gives:

$$(L_1, L_2, L_3, L_t) = \frac{(\sin(\theta_1 + \theta_2) * \sin(\theta_2 + \theta_t))}{(\sin(\theta_1 + \theta_2 + \theta_t) * \sin \theta_2)}.$$

Using the fact that  $(L_1, L_2, L_3, L_t) = c$ , the equation can be rewritten as follows:

$$(c-1)\sin \theta_2 \cos \theta_t + \left( \frac{c \sin \theta_2}{\tan(\theta_1 + \theta_2)} - \cos \theta_2 \right) \sin \theta_t = 0.$$

This equation in  $\theta_t$  is solved using the change of variable

$g = \tan \frac{\theta_t}{2}$ . Note that there are in general 2 solutions to this equation. However, these solutions are equal modulo  $\pi$ , so that they define the same line  $L_t$ .

The needle is rotated by angle  $\theta_t$  from position  $L_3$  to  $L_t$ .

This achieves visual servoing. At position  $L_t$ , the needle is visually aligned to the target in the 2D image.

Note that only visual alignment is achieved. Unless the 3D target  $T$  belongs to plane  $\Pi$ , full 3D alignment is not achieved. As shown in section 2, complete 3D alignment

can be obtained only by performing visual servoing of the needle in several successive planes.

Note that this visual servoing technique does not require any camera calibration. It also converges in exactly three iterations, contrary to most visual servoing approaches, which require a variable and often larger number of iterations. This is important in X-ray applications where each new image increases the radiation exposure of both patient and surgeon.

This visual servoing approach can be applied to any imaging device that can be approximated by a pinhole camera. In applications where the number of iterations is not critical, precision can be improved by considering  $n > 3$  successive needle positions  $L_1, L_2, \dots, L_n$ . Then  $\theta_t$  can then be estimated by least-square approximation from all the possible cross-ratios between lines  $L_1, L_2, \dots, L_n$ .

#### 4. Insertion Depth Calculation using cross-ratios

Once the needle is aligned to the 3D target using the combination of approaches presented in section 2 and 3, we also estimate the necessary depth of insertion. Our method is based on the invariance of cross-ratios to perspective projections. The method is the following:

We use two markers  $M_1, M_2$  aligned with the line of the needle. These can be metallic balls mounted on a needle guide.  $M_1, M_2$  project into the image onto 2D points  $m_1, m_2$ .

$f$  is the projection of the fixed entry point  $F$ .  $F$  also corresponds to the tip of the needle before insertion.  $t$  is the projection of 3D target  $T$  in the image. Since the needle has already been aligned to the target in 3D,  $T, F, M_1, M_2$  are aligned. According to projective geometry, the cross-ratio of the 3D points,  $T, F, M_1, M_2$  is equal to the cross-ratio of their projections in the image, e.g.:

$$(M_1, M_2, F, T) = (m_1, m_2, f, t) = \lambda.$$

The cross-ratio  $\lambda = (m_1, m_2, f, t) = \frac{\|ft\| * \|m_1 m_2\|}{\|m_2 t\| * \|m_1 f\|}$  can

be measured in the image. The Euclidean distances

between the 3D points  $F$ ,  $M_1, M_2$  can be measured on the needle. Therefore the insertion depth  $\|FT\|$  necessary to reach the target from entry point  $F$  can be estimated as follows:

$$\|FT\| = \frac{\lambda * \|M_1 F\| * \|M_2 F\|}{\|M_1 M_2\| - \lambda * \|M_1 F\|}.$$

In practice, if possible, more markers can be used to get more precision.

Note that aligning the needle to the target (section 2 and 3) and estimating insertion depth (this section) completely determines the three-dimensional position of the target. Thus, by successively “targeting” two 3D points inside the patient, we can estimate metric distances between anatomical structures. This is illustrated by fig. 6. This could be used for instance to determine the distance between a tumor to be removed and the nearest major blood vessel prior to surgery, in order to assess the risk associated with it. The interest of using our procedure to do this is that it is quick and uses a cheap and readily available imaging modality (the X-ray). A tomographic reconstruction of a volume of the patient’s body would provide the same information, but would be more costly.

## 5. Experimental Results

### 5.1 Test of the technique for visual servoing of a needle in a plane

To test our approach for visual servoing of a needle in a plane (presented in section 3), we used a protractor placed on an inclined plane. It was viewed from approximately a three-quarter view by a camera (see fig. 5). The pendulum of the protractor was photographed at four different positions. The first three positions are assumed to be known and correspond to the following angles:  $\alpha_1 = 30^\circ$ ,  $\alpha_2 = 90^\circ$  and  $\alpha_3 = 150^\circ$ . We assume the fourth position  $\alpha_t$  to be unknown. The corresponding positions  $l_i$  of the pendulum inside edge in the image are measured. Since this edge goes through the pendulum’s center of rotation, we can apply our visual servoing approach. The intersections of the lines  $l_i$  with an arbitrary line  $m$  are:  $q_1 = (223,184), q_2 = (310,253), q_3 = (411,333), q_t = (269,221)$

The cross-ratio of these 4 points is:  $c = -1.64$ . We apply the final equation of section 3:

$$(c-1)\sin\theta_2 \cos\theta_t + \left( \frac{c \sin\theta_2}{\tan(\theta_1 + \theta_2)} - \cos\theta_2 \right) \sin\theta_t = 0 \quad \text{with}$$

$$\theta_1 = \alpha_2 - \alpha_1 = 60^\circ, \theta_2 = \alpha_3 - \alpha_2 = 60^\circ. \quad \text{This gives:}$$

$-2.29 * \cos\theta_t + 0.32 * \sin\theta_t = 0$ . This equation has 2 solutions:  $\theta_t = 82.03^\circ$  and  $\theta_t = -97.97^\circ$  (equal modulo  $\pi$ ). They correspond to the same 3D line position  $\alpha_t = 52.03^\circ$ . Given that the true value is  $\alpha_t = 52^\circ$ , this experiment shows that our approach for visual servoing of a needle rotating in a plane is accurate, despite the fact that it requires only 3 iterations (e.g. three rotations of the needle:  $\alpha_1 \rightarrow \alpha_2 \rightarrow \alpha_3 \rightarrow \alpha_t$ ).

### 5.2 Test of the precision of needle 3D alignment

We tested the approach for 3D needle alignment presented in section 2 on images showing 1) only a needle and metal ball targets 2) on medical images showing a pig kidney.

#### Set-ups:

For our experiments we used three different medical robots to hold the needle: LARS (IBM Research), RCM (university design) and Neuromate (Integrated Surgical Systems). These robots have different characteristics in size, kinematics, working volume and speed of motion. Neuromate is the only one that has the approval of the Food and Drug Administration for automated surgery.

For image acquisition, we used a CCD-camera in one experiment and a uniplanar X-ray fluoroscope (C-arm) in another one. For the CCD-camera we built a C-arm simulator. We fixed a CCD camera on one end of the C-arm simulator and a piece of white foam cored carton on the other end. This provides us with a “white background” in the image. Thus, we obtained quite similar images, both in the CCD- and in the X-ray-scenario.

#### Results:

For our first experiments, we used the CCD-camera and the LARS robot (see fig. 6). Targets were small black balls with a diameter of 4mm. The distance between needle tip and the targets was approximately 60mm. 60 different automatic target alignment experiments were conducted. We computed the deviation vector as the distance of the target to the axis of the needle. The mean and maximum deviations were 0.21 and 0.38 millimeters. The mean error in estimated insertion depth was 1.2mm.

In the second experiment, we used a small uniplanar X-ray fluoroscope with an approximate source to intensifier distance of 1 meter, and an intensifier diameter of about 14cm. This time the needle was moved by the RCM robot. The target was a metal ball of 4mm in diameter and it was

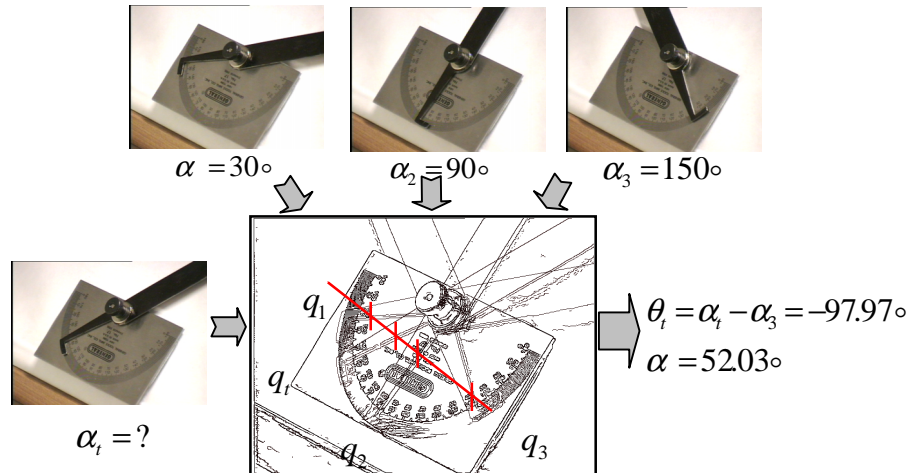


**Figure 5 – This experiment illustrates our technique for visual servoing of a needle in a plane. It estimates the 3D rotation angle that must be applied to the pendulum of a protractor so that it reaches a given position in the image by: 1) rotating the pendulum by 2 arbitrary angles 2) measuring in the image the cross-ratio between the 3 successive positions of the pendulum and the desired position. The 3D rotation angle is then a simple function of the cross-ratio value.**

positioned at about 70mm away from the needle tip. The images were small and of poor quality. However, the mean deviation of the needle after the alignment process was about 1.5mm, which is quite satisfactory. We do not show images of this experiment here, due to lack of space.

In the third experiment, we performed a puncture on a pig kidney. The needle was manipulated by the RCM-robot. We injected contrast in a blood vessel of the kidney before puncture. The user interface in the background shows the X-ray image. We used a small GE mobile X-ray C-arm (GE Polarix 2) for image acquisition. The target of the puncture is the first main intersection of the contrasted blood vessel of the pig kidney. We used our approach to align the needle to the 3D target. The needle was then inserted. As shown by fig. 7, the needle reached the chosen target. This proves that our approach correctly aligned the needle to the target. Note that, in this example, the insertion depth was not calculated automatically. The user used the X-ray image to guide the robot to insert to the required depth.

These experiments show the accuracy of our approach for 3D needle alignment by visual servoing (see section 2 and 3) and estimation of insertion depth. Future work involves more clinical tests.

## 6. Conclusion

This paper proposes a simple and accurate method for needle placement. This approach uses new visual servoing techniques based on projective geometry and perspective invariants. The only human interaction required by the

system is the choice of the needle entry point on the patient and the manual definition of the target point on a computer display showing the X-ray images of two arbitrary views. Our method requires no additional sensors (infrared, laser, ultrasound, MRI, and etc), no stereotactic frame and no prior calibration using a phantom or fiducial markers. The approach has been tested using different robots to hold the needle and using a CCD-camera and a uniplanar X-ray fluoroscope as imaging systems. Promising first results present this method as a serious alternative to other needle placement techniques, which require cumbersome and time consuming calibration procedures.

## 7. References

- [1] J.R. Adler, A.Schweikard, R.Tombropoulos, and J.C. Latombe. "Image guided robotic radiosurgery." *First Internat. Symposium on Medical Robotics and Computer-Assisted Surgery*, pages 291--297, Pittsburgh, September 1994.
- [2] E.Bainville, P.Chaffanjon, and P.Cinquin. "Computer generated visual assistance to a surgical operation: the retroperitoneoscopy." *First Internat. Symposium on Medical Robotics and Computer-Assisted Surgery*, pages 254--257, Pittsburgh, September 1994.
- [3] H.Behnke, F.Bachmann, K.Fladt, and H.Kunle. "From Projective to Euclidean Geometry", volume 2, MIT Press, Cambridge, MA, and London, UK, 1986.
- [4] P.I. Croke. "Visual control of robot manipulators - a review." In *Visual Servoing*, pages 1-31, World Scientific, 1993.

[5] B.Davey, P.Munger, R.Comeau, L.Pisane, A.Olivier, and T.Peters. "Applying stereoscopic visualization to image guided neurosurgery". *First Internat. Symposium on Medical Robotics and Computer-Assisted Surgery*, pages 264--271, Pittsburgh, September 1994.

[6] S.Lavallee, P.Sautot, J.Troccaz, P.Cinquin, and P.Merloz. "Computer assisted spine surgery: a technique for accurate transpedicular screw fixation using CT data and a 3D optical localizer." *First Internat. Symposium on Medical Robotics and Computer-Assisted Surgery*, pages 315--322, Pittsburgh, September 1994.

[7] P.Potamianos, B.L. Davies, and R.D.Hibberd. "Intra-operative imaging guidance for keyhole surgery methodology and calibration." *First Internat. Symposium on Medical Robotics and Computer-Assisted Surgery*, pages 98--104, Pittsburgh, September 1994.

[8] A. Bzostek, A.C. Barnes, R. Kumar, J.H. Anderson, R.H. Taylor. "A Testbed System for Robotically Assisted Percutaneous Pattern Therapy". In Proc. of Medical Image Computing and Computer-Assisted Intervention (MICCAI'99), Cambridge, UK, Sept. 1999.

[9] O.D. Faugeras. "Three-Dimensional Computer Vision: A Geometric Viewpoint", MIT Press, 1993.

[10] E. Malis, F. Chaumette, S. Boudet. - "2 1/2 D Visual Servoing" - IEEE Trans. on Robotics and Automation, 15(2):238-250, Avril 1999.

[11] D. Stoianovici, L.L. Whitcomb, J.H. Anderson, R.H. Taylor and L.R. Kavoussi. "A Modular Surgical Robotic System for Image Guided Percutaneous Procedures". In Proc. of Medical Image Computing and Computer-Assisted Intervention (MICCAI'98), Cambridge, MA, USA, Oct. 1998.

[12] N. Navab and B. Geiger, "Apparatus and method for positioning a biopsy needle", US Patent Application, filed Sep. 30, 1996. Serial No. 08/722,725. and "Apparatus and method for point reconstruction and metric measurement on radiographic images", US Patent 6,028,912, <http://www.uspto.gov/patft/index.html>.

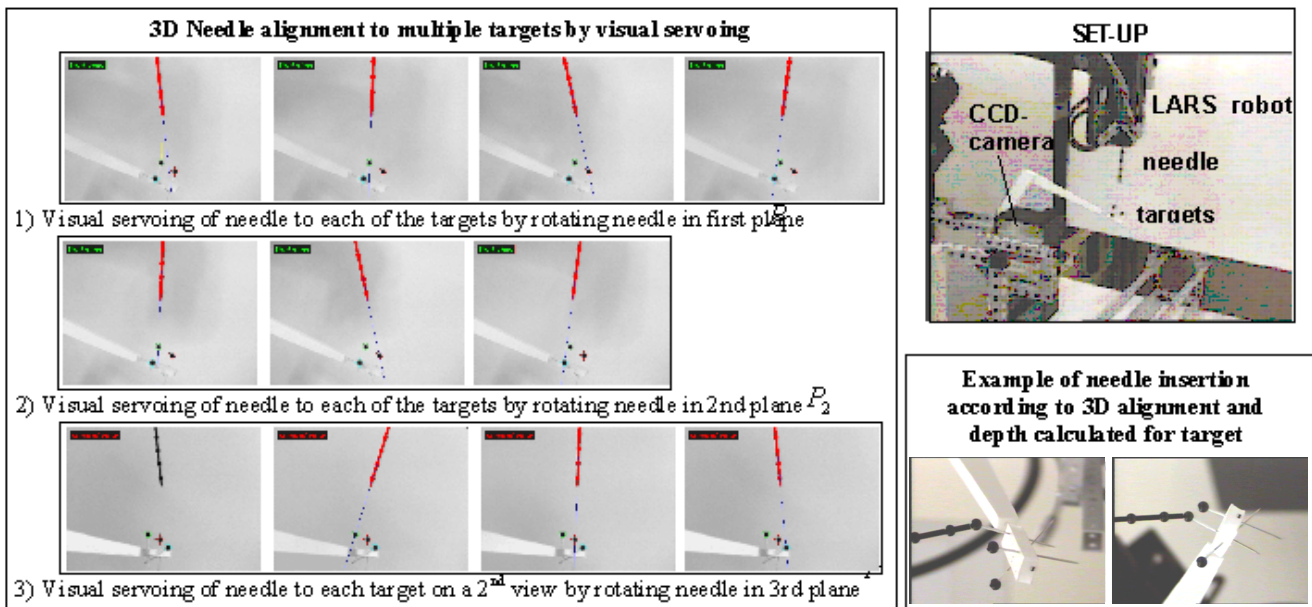
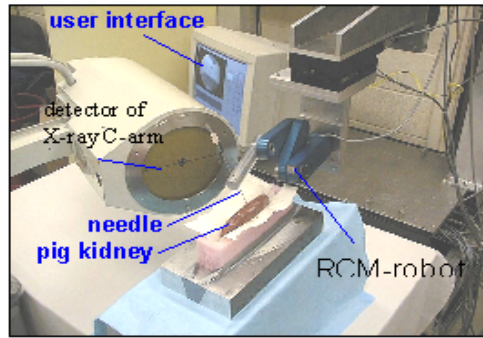
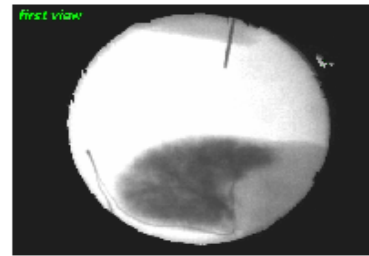


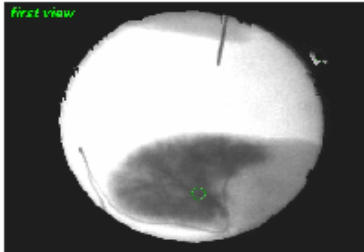
**Figure 6 – This figure shows the 3D alignment of a needle with three different target points using our approach. The 4 marker balls fixed on the needle phantom are used to estimate the insertion depth needed for each target. Insertion of the needle to one of the targets illustrates the precision of the alignment and depth calculation. At the end of this process, the 3D position of each target is entirely determined. As a consequence, it is possible to estimate the Euclidean distances between the 3D target points. Note that here we used a CCD-camera for image acquisition.**



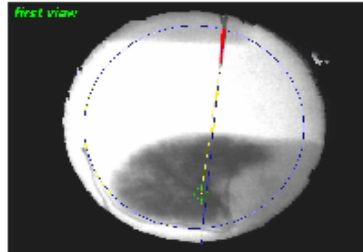
Experimental set-up



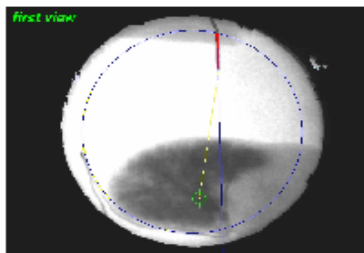
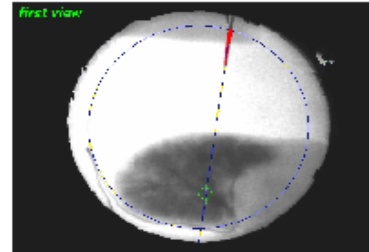
First X-ray view



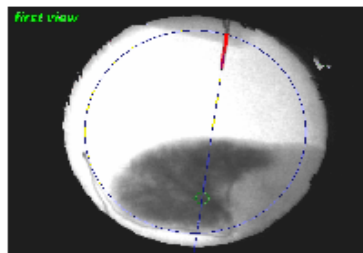
Target defined by surgeon



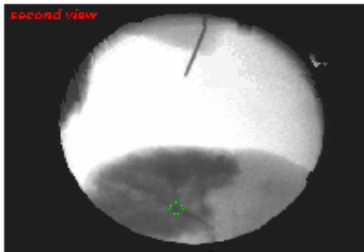
Visual servoing of needle to target by rotating needle in first plane



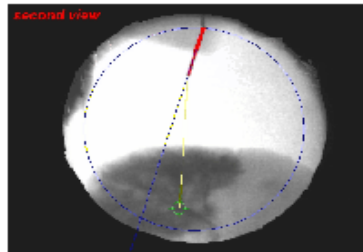
Visual servoing of needle to target by rotating needle in second plane<sup>1,2</sup>



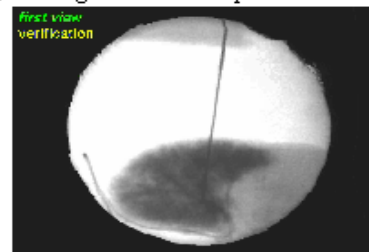
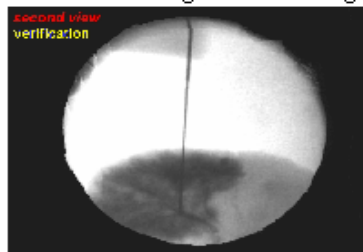
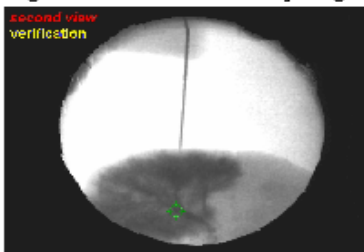
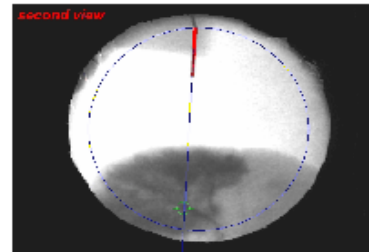
Second X-ray view



Target re-defined in 2<sup>nd</sup> view by surgeon



Visual servoing of needle to target by rotating needle in third plane



Needle insertion

Return to first view after needle insertion

Figure 7 - Pig-kidney puncture test using our needle alignment method by visual servoing. The needle is manipulated by the RCM-robot. We contrasted a blood vessel of the kidney before puncture. X-ray images are taken by a small mobile X-ray C-arm. The needle is successfully aligned with the first main intersection of the contrasted blood vessel of the pig kidney. This is illustrated by the fact that after insertion the needle reaches the designated area.